blood®
Plenary Paper

RED CELLS, IRON, AND ERYTHROPOIESIS

Lobe specificity of iron binding to transferrin modulates murine erythropoiesis and iron homeostasis

Nermi L. Parrow,[1] Yihang Li,[1] Maria Feola,[2] Amaliris Guerra,[3] Carla Casu,[3] Princy Prasad,[1] Luke Mammen,[1] Faris Ali,[1] Edvinas Vaicikauskas,[1] Stefano Rivella,[3,*] Yelena Z. Ginzburg,[2,*] and Robert E. Fleming[1,4,*]

[1]Department of Pediatrics, Saint Louis University School of Medicine, St. Louis, MO; [2]Division of Hematology-Oncology, Icahn School of Medicine at Mount Sinai, New York, NY; [3]Division of Hematology, Department of Pediatrics, Children's Hospital of Philadelphia, Philadelphia, PA; and [4]Edward A. Doisy Department of Biochemistry and Molecular Biology, Saint Louis University School of Medicine, St. Louis, MO

KEY POINTS

- Iron occupancy of the N compared with C lobe of transferrin confers functionally distinct properties.
- The monoferric forms of transferrin influence hepcidin expression and erythropoietin responsiveness.

Transferrin, the major plasma iron-binding molecule, interacts with cell-surface receptors to deliver iron, modulates hepcidin expression, and regulates erythropoiesis. Transferrin binds and releases iron via either or both of 2 homologous lobes (N and C). To test the hypothesis that the specificity of iron occupancy in the N vs C lobe influences transferrin function, we generated mice with mutations to abrogate iron binding in either lobe ($Tf^{N\text{-}bl}$ or $Tf^{C\text{-}bl}$). Mice homozygous for either mutation had hepatocellular iron loading and decreased liver hepcidin expression (relative to iron concentration), although to different magnitudes. Both mouse models demonstrated some aspects of iron-restricted erythropoiesis, including increased zinc protoporphyrin levels, decreased hemoglobin levels, and microcytosis. Moreover, the $Tf^{N\text{-}bl/N\text{-}bl}$ mice demonstrated the anticipated effect of iron restriction on red cell production (ie, no increase in red blood cell [RBC] count despite elevated erythropoietin levels), along with a poor response to exogenous erythropoietin. In contrast, the $Tf^{C\text{-}bl/C\text{-}bl}$ mice had elevated RBC counts and an exaggerated response to exogenous erythropoietin sufficient to ameliorate the anemia. Observations in heterozygous mice further support a role for relative N vs C lobe iron occupancy in transferrin-mediated regulation of iron homeostasis and erythropoiesis. (*Blood*. 2019;134(17):1373-1384)

Introduction

Transferrin (Tf), the major iron-binding glycoprotein in serum, participates in iron homeostasis as an iron cargo molecule and signaling ligand.[1,2] Tf receptors 1 (TfR1) and 2 (TfR2) have distinct distributions and characteristics that may provide a plausible basis for these distinct roles. How the iron-binding and signaling properties of Tf interrelate is unclear. An ancient gene duplication gave rise to the Tf bilobed structure,[3] with each lobe (N and C) binding (and releasing) 1 molecule of iron.[4] As such, Tf circulates in 4 forms: diferric, monoferric N lobe, monoferric C lobe, and apotransferrin.[5] Under physiologic conditions, Tf is not fully saturated with iron, and most of the serum iron-containing Tf is monoferric.[6] However, because diferric Tf has a much greater affinity for TfR1 than does monoferric, the latter forms contribute minimally to cellular iron delivery under physiologic conditions.[7] In iron deficiency, a shift away from diferric and toward monoferric forms of Tf makes TfR1 occupancy by the monoferric forms increasingly relevant. Although the monoferric forms deliver 1 iron molecule per endocytic cycle rather than 2, cellular iron depletion results in a compensatory increase in TfR1 expression.[8]

TfR1 is thought to function primarily as an iron cargo receptor, although it has been reported to participate in signaling in some circumstances.[9,10] In contrast, TfR2 seems to mediate signaling events that regulate iron metabolism and erythropoiesis. Hepatocellular TfR2 regulates hepcidin expression, and its loss leads to hemochromatosis.[11,12] TfR2 is also expressed in erythroid precursors,[13] where it modulates erythropoiesis,[14,15] possibly as a component of the erythropoietin (Epo)–Epo receptor (EpoR) complex.[14] One report suggests that TfR2 acts as a chaperone, bringing the EpoR to the cell surface, and thus functions to increase Epo sensitivity[14]; others demonstrate that TfR2 is necessary for attenuation of erythroblast Epo sensitivity under iron-restricted conditions.[15,16] Diferric Tf participates in TfR2-mediated signaling events.[2,17-19] However, the mechanism by which diferric Tf, at concentrations (micromolar) far higher than the binding constant for TfR2 (nanomolar), could serve as a physiologic signaling ligand is unclear.[20] Plausibly, the lower affinity of diferric Tf for TfR2 compared with TfR1[21] might permit monoferric forms to compete with diferric Tf for TfR2 occupancy under physiologic conditions. If the signaling consequences of the monoferric forms differed from those of diferric Tf, a mechanism for regulating TfR2-mediated events would be provided. Supporting this possibility is the observation that administration of exogenous apotransferrin modulates erythropoiesis in $Hbb^{th1/th1}$ (β-thalassemic) mice.[22]

To investigate the potential contribution of monoferric Tfs in the regulation of iron metabolism and erythropoiesis, we generated mice in which either the N or C lobe was blocked ($Tf^{N\text{-}bl/N\text{-}bl}$ and $Tf^{C\text{-}bl/C\text{-}bl}$; ie, unable to bind iron). The mutant mice had evidence of decreased erythroblast iron delivery, with elevated zinc protoporphyrin levels and microcytic anemia. Identifying a role for Tf in modulating Epo sensitivity, the $Tf^{C\text{-}blC\text{-}bl}$ but not $Tf^{N\text{-}bl/N\text{-}bl}$ mice demonstrated increased red blood cell (RBC) counts and an exaggerated response to exogenous Epo. Consistent with participation of Tf in regulating hepcidin, the $Tf^{N\text{-}bl/N\text{-}bl}$ and $Tf^{C\text{-}bl/C\text{-}bl}$ mice had relatively decreased hepcidin levels and liver iron overload, but to different degrees. Mice heterozygous for each Tf mutation had subtle phenotypic differences from wild-type (WT) mice and from each other, further supporting distinct regulatory roles for the 2 monoferric Tf forms in iron metabolism and erythropoiesis.

Methods

Mouse models

Transgenic mice producing modified Tf unable to bind iron in either the N or C lobe were generated on a C57BL/6 background by site-directed mutagenesis of the nucleotides encoding 2 essential tyrosines in the iron-binding sites of each of the lobes to instead encode phenylalanine.[23] For the $Tf^{N\text{-}bl/N\text{-}bl}$ mutant strain, A to T nucleotide substitutions resulted in Y114F and Y207F, and for the $Tf^{C\text{-}bl/C\text{-}bl}$ mutant strain, A to T substitutions resulted in Y448F and Y537F. Chimeric mice were generated commercially (Cyagen Biosciences, Santa Clara, CA). Founders were bred in the animal facility at Saint Louis University. Mice were group housed by sex, fed standard chow (200 ppm of iron) ad libitum, and maintained on 12-hour light cycles. Experiments were performed on 8- to 10-week-old mice. Animal studies were performed under Institutional Animal Care and Use Committee–approved protocols.

Genotyping

Polymerase chain reaction (PCR) was performed with RedTaq ReadyMix PCR reaction mix (Sigma, St. Louis, MO) per manufacturer's instructions. Primer sequences were as follows: $Tf^{N\text{-}bl/N\text{-}bl}$, forward 5′-TGTAGGCAGGTAGCCGACATTAGAA and reverse 5′-TTCTCTTGTCCATGGCGCCT; $Tf^{C\text{-}bl/C\text{-}bl}$, forward 5′-ATGGCT CCATAGGAGCTGTGCA and reverse 5′-GCCATCCCACCTCAT TCCTTAGCT. Thermal cycling (at 94°C for 2 minutes followed by 32 cycles at 94°C for 30 seconds, 60°C for 30 seconds, and 72°C for 30 seconds and a final 7-minute extension at 72°C).

Hematologic and serum iron parameters

Complete blood counts were measured by the Cell-Dyn 3700 analyzer (Advanced Veterinary Laboratories, St. Louis, MO). Serum iron, total iron-binding capacity (TIBC), and unsaturated iron-binding capacity (UIBC) were assayed (Pointe Scientific, Canton, MI) per manufacturer's protocol. Tf saturation was calculated as serum iron/TIBC × 100, with TIBC calculated from UIBC. Tf concentrations, serum hepcidin, and serum Epo were assayed by enzyme-linked immunosorbent assay (Abcam, Cambridge, MA; Intrinsic Life Sciences, LaJolla, CA; and R&D Systems, Minneapolis, MN, respectively).

Flow cytometry

Erythroid populations were analyzed by flow cytometry as previously described.[24,25] Antibodies and gating strategies are described in supplemental Figure 7 (available on the *Blood* Web site). For phosphorylated AKT (pAKT) analyses, cells were permeabilized and fixed with the Flow Cytometry Fixation and Permeabilization Buffer Kit (R&D Systems). Apoptosis was measured with the PE Annexin V Apoptosis Detection Kit (BD Biosciences).

RBC lifespan

Mice were injected retroorbitally with Sulfo-NHS-Biotin (ThermoFisher; category No. 21217). The following day, 1×10^6 RBCs were stained with a streptavidin-phycoerythrin antibody (BD Pharmingen). Percentage of biotinylation was monitored twice per week for 14 days and then once per week until day 34. Data were analyzed with FlowJo 10.2 software (Tree Star, Inc., Ashland, OR).

Zinc protoporphyrin assays

The fraction of protoporphyrin containing zinc was assayed from whole blood using an AVIV hematoflourometer (AVIV Biomedical, Lakewood, NJ).

NTBI measurements

Non–Tf-bound iron (NTBI) was quantified by a nitrilotriacetic acid ultrafiltration assay as previously described.[26] Briefly, serum was incubated with nitriloacetic acid, and proteins were then depleted from the sample by ultrafiltration (NanoSep; Pall Corporation, Port Washington, NY) with centrifugation at 10 620 ×*g* for 45 minutes at 15°C. Iron was measured from the resulting filtrate by colorimetric assay.[27]

Epo responsiveness

Mice were treated by intraperitoneal injection with 3000 IU/kg per day of recombinant human Epo (Procrit; Janssen Biotech, Raritan, NJ) or normal saline (Baxter, Deerfield, IL) for 4 consecutive days. Hematologic parameters were measured on the fifth day.

Tissue iron concentrations

Tissue iron concentrations were determined as previously described.[28]

Quantitative reverse transcription PCR

Tissue samples were homogenized in guanidinium thiocyanate (Trizol; Ambion, Carlsbad, CA), and RNA was extracted per manufacturer's protocol. RNA was reverse transcribed with iScript RT supermix (Biorad, Hercules, CA), and quantitative reverse transcription PCR was performed with Taqman Gene Expression assay primers and probes (Applied Biosystems, Foster City, CA). Thermal cycling (at 95°C for 15 seconds and 60°C for 1 minute for 40 cycles) was performed with a CFX Connect real-time system (Biorad). Data were analyzed by the $-\Delta$Ct method.[29]

Histology

Tissues were fixed and stained by the Perls' Prussian blue method with or without enhancement with diaminobenzidine as previously described.[30]

Statistical analyses

Statistical analyses were performed in GraphPad Prism 7. Outliers identified by the ROUT method were excluded. Data were analyzed by analysis of variance (ANOVA), Student *t* test,

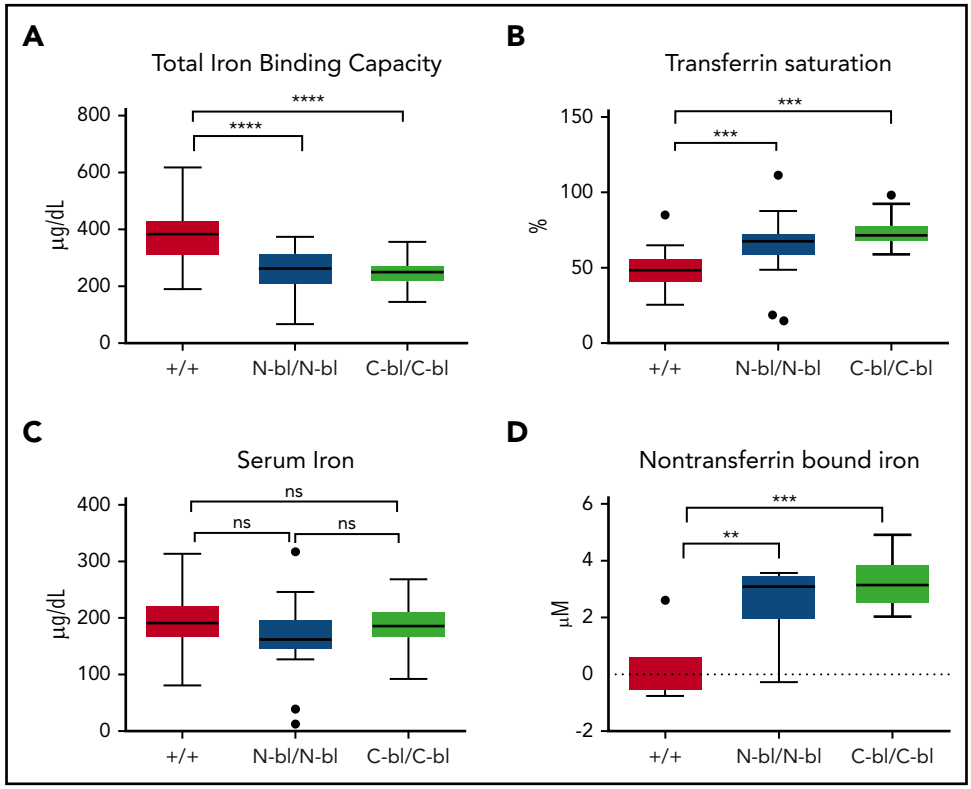

Figure 1. Mutation of the individual Tf lobes increases Tf saturation without altering serum iron. (A) Total iron-binding capacity was decreased upon loss of iron binding to either lobe of Tf compared with WT. (B) Tf saturations in $Tf^{N\text{-}bl/N\text{-}bl}$ and $Tf^{C\text{-}bl/C\text{-}bl}$ mice were significantly higher than those in WT but not significantly different from each other. (C) No significant differences in serum iron concentrations were observed across the 3 strains. For panels A-C, n = 14 mice per sex for WT and 7 to 8 males and 13 females per group for mutant mice, respectively. (D) Both $Tf^{N\text{-}bl/N\text{-}bl}$ and $Tf^{C\text{-}bl/C\text{-}bl}$ mice demonstrated increased non–Tf-bound iron concentrations compared with WT. For panel D, n = 2 to 3 female mice per group and n = 4 to 5 male mice per group. Data are presented as Tukey box and whisker plots. Statistical significance was analyzed by ANOVA. $^{**}P \leq .01$, $^{***}P \leq .001$, $^{****}P \leq .0001$. ns, nonsignificant.

or Kruskal-Wallis test, with $P < .05$ considered statistically significant.

Results

Abrogation of iron binding to either lobe increases Tf saturation without altering serum iron or Tf concentration

Mice producing Tfs unable to bind iron in the N or C lobe were generated by mutating 2 essential tyrosines in the iron-binding site of each of the lobes[23] (supplemental Figure 1). Mutant mice seemed healthy and were fertile and without overt abnormalities or evident differences between strains in body weight or splenic weight indexed to body weight (supplemental Figure 2). High-performance liquid chromatography analyses of serum from the mutant mice supported the absence of diferric Tf and presence of the expected monoferric forms (data not shown). Initial experiments focused on defining the effects of C- and N-blocked Tf on circulating iron parameters. Because each mutant strain had 1 blocked iron-binding site, $Tf^{N\text{-}bl/N\text{-}bl}$ and $Tf^{C\text{-}bl/C\text{-}bl}$ mice exhibited a decrease in TIBC (Figure 1A) and increase in calculated Tf saturation compared with WT mice (Figure 1B). Tf concentrations were not different between strains (supplemental Figure 3A). Accordingly, UIBC was lower in $Tf^{N\text{-}bl/N\text{-}bl}$ and $Tf^{C\text{-}bl/C\text{-}bl}$ mice relative to WT (supplemental Figure 3B). There were no significant differences in serum iron between the 3 strains (Figure 1C). $Tf^{N\text{-}bl/N\text{-}bl}$ and $Tf^{C\text{-}bl/C\text{-}bl}$ mice demonstrated NTBI in the plasma (Figure 1D), as anticipated in the setting of high Tf saturation.[31] Thus, $Tf^{N\text{-}bl/N\text{-}bl}$ and $Tf^{C\text{-}bl/C\text{-}bl}$ mice demonstrated expected changes in iron-binding capacity relative to WT mice, but without evident differences in circulating iron status between the mutant strains.

Lobe specificity of Tf iron binding differentially affects circulating red cell indices

Evidence supports roles for erythroid TfRs in iron delivery and erythroblast hemoglobinization and differentiation.[15,32,33] We therefore analyzed the effect of lobe-specific Tf iron occupancy on multiple erythroid parameters. Although hemoglobin (Hb) concentrations were lower in both mutant strains relative to WT mice, $Tf^{N\text{-}bl/N\text{-}bl}$ mice had significantly lower Hb concentrations relative to $Tf^{C\text{-}bl/C\text{-}bl}$ mice (Figure 2B). Strikingly, $Tf^{C\text{-}bl/C\text{-}bl}$ mice had significantly higher RBC counts relative to both $Tf^{N\text{-}bl/N\text{-}bl}$ and WT mice (Figure 2A), despite a mild microcytic anemia in both strains (Figure 2B-D). MCV values were lower in the mutant strains relative to WT, with significantly more microcytic cells in the $Tf^{C\text{-}bl/C\text{-}bl}$ mice relative to the $Tf^{N\text{-}bl/N\text{-}bl}$ mice (Figure 2C). MCH levels corresponded to MCV values, with both mutant strains decreased relative to WT; however, a significantly more pronounced decrease was observed in the $Tf^{C\text{-}bl/C\text{-}bl}$ relative to the $Tf^{N\text{-}bl/N\text{-}bl}$ mice (Figure 2D). No significant differences in mean corpuscular Hb concentrations were found (Figure 2E). Despite lower MCVs, the increase in RBC counts was sufficient to produce a higher hematocrit in $Tf^{C\text{-}bl/C\text{-}bl}$ relative to the $Tf^{N\text{-}bl/N\text{-}bl}$ mice, although both remained significantly lower than WT (supplemental Figure 4A). Both mutant strains exhibited an increase in red cell distribution width compared with WT mice (supplemental Figure 4C). $Tf^{N\text{-}bl/N\text{-}bl}$ mice showed a modest increase in reticulocyte counts relative to WT mice but not $Tf^{C\text{-}bl/C\text{-}bl}$ mice (supplemental Figure 4B). The increased RBC counts in the $Tf^{C\text{-}bl/C\text{-}bl}$ mice were not mediated by alterations in RBC lifespan, because they were not significantly different across strains (Figure 2F). Collectively, these data demonstrate that iron binding to the N lobe of Tf (and/or loss of C-lobe binding) in the $Tf^{C\text{-}bl/C\text{-}bl}$ mice resulted in increased RBC production and less

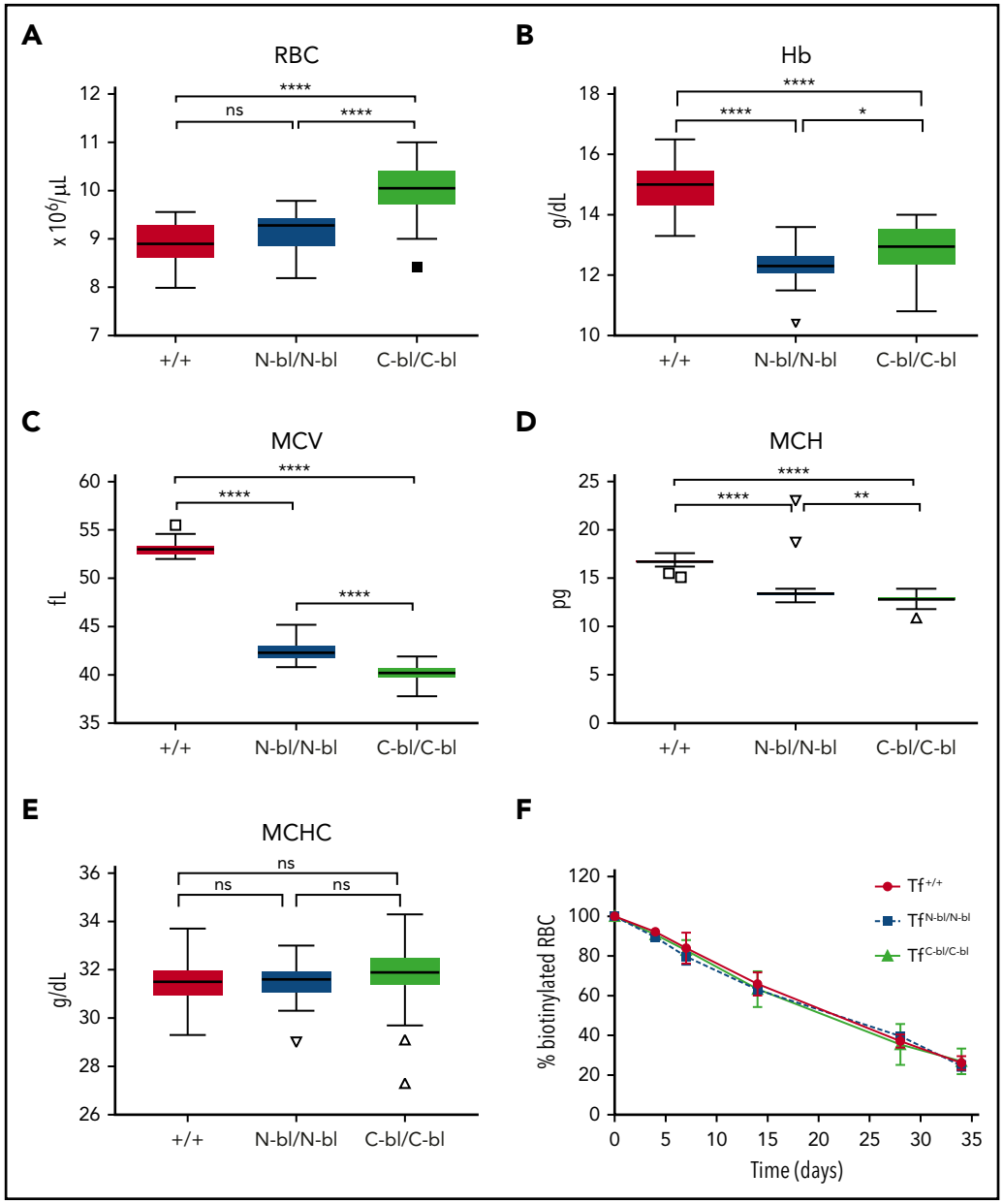

Figure 2. Iron binding to different lobes of Tf differentially affects red cell indices. Complete blood count (CBC) parameters from 2-month-old mice demonstrated significant increases in RBCs in the $Tf^{C\text{-}bl/C\text{-}bl}$ mice relative to $Tf^{N\text{-}bl/N\text{-}bl}$ and WT mice (A), significant decreases in Hb concentration in both the $Tf^{N\text{-}bl/N\text{-}bl}$ and $Tf^{C\text{-}bl/C\text{-}bl}$ mice relative to WT, with more pronounced decreases in the $Tf^{N\text{-}bl/N\text{-}bl}$ mice (B), significant decreases in mean corpuscular volume (MCV) in both the $Tf^{N\text{-}bl/N\text{-}bl}$ and $Tf^{C\text{-}bl/C\text{-}bl}$ mice relative to WT, with more pronounced microcytosis in the $Tf^{C\text{-}bl/C\text{-}bl}$ strain (C), significant decreases in mean cellular Hb (MCH) in the $Tf^{N\text{-}bl/N\text{-}bl}$ and $Tf^{C\text{-}bl/C\text{-}bl}$ mice relative to WT, with more pronounced decreases in the $Tf^{C\text{-}bl/C\text{-}bl}$ mice (D), and no significant differences in mean corpuscular Hb concentration (MCHC) between strains (E). (F) Red cell lifespan assays, measuring the decrease in the percentage of biotinylated red cells over time, indicated no differences between strains. Data are presented as Tukey box and whisker plots or line graphs, with mean ± standard deviation values indicated for each time point. For CBC parameters, n = 13 to 18 females and 13 to 17 males per strain. For red cell lifespan assays, n = 3 to 6 mice per sex for WT and n = 3 to 4 mice per sex for mutant mice. Statistical significance was analyzed by Kruskal-Wallis or 1-way ANOVA for hematologic parameters and 2-way ANOVA with Geisser-Greenhouse correction for lifespan data. $*P \leq .05$, $**P \leq .01$, $****P \leq .0001$.

pronounced anemia (despite increased microcytosis) relative to $Tf^{N\text{-}bl/N\text{-}bl}$ mice.

Monoferric N and C Tfs demonstrate similar iron availability for heme but differential effects on erythropoiesis

Differences in RBC count between the Tf-mutant strains led us to investigate participants in erythropoietic signaling. Lack of iron binding to the N lobe of Tf resulted in increased serum Epo compared with loss of iron binding to the C lobe or WT (Figure 3A), consistent with changes in Hb concentrations. mRNA expression of the erythroid marker, glycophorin A,[34] was increased in bone marrow from $Tf^{C\text{-}bl/C\text{-}bl}$ mice, but not $Tf^{N\text{-}bl/N\text{-}bl}$ mice, relative to WT mice (Figure 3B). Expression of Erfe, a hepcidin regulator produced by erythroblasts in response to Epo,[35] was significantly higher in both mutant strains compared with control mice (Figure 3C). However, when Erfe expression was normalized to GypA expression, only $Tf^{C\text{-}bl/C\text{-}bl}$ mice exhibited a significant increase relative to controls (Figure 3D). Serum Erfe levels in the mutant and WT

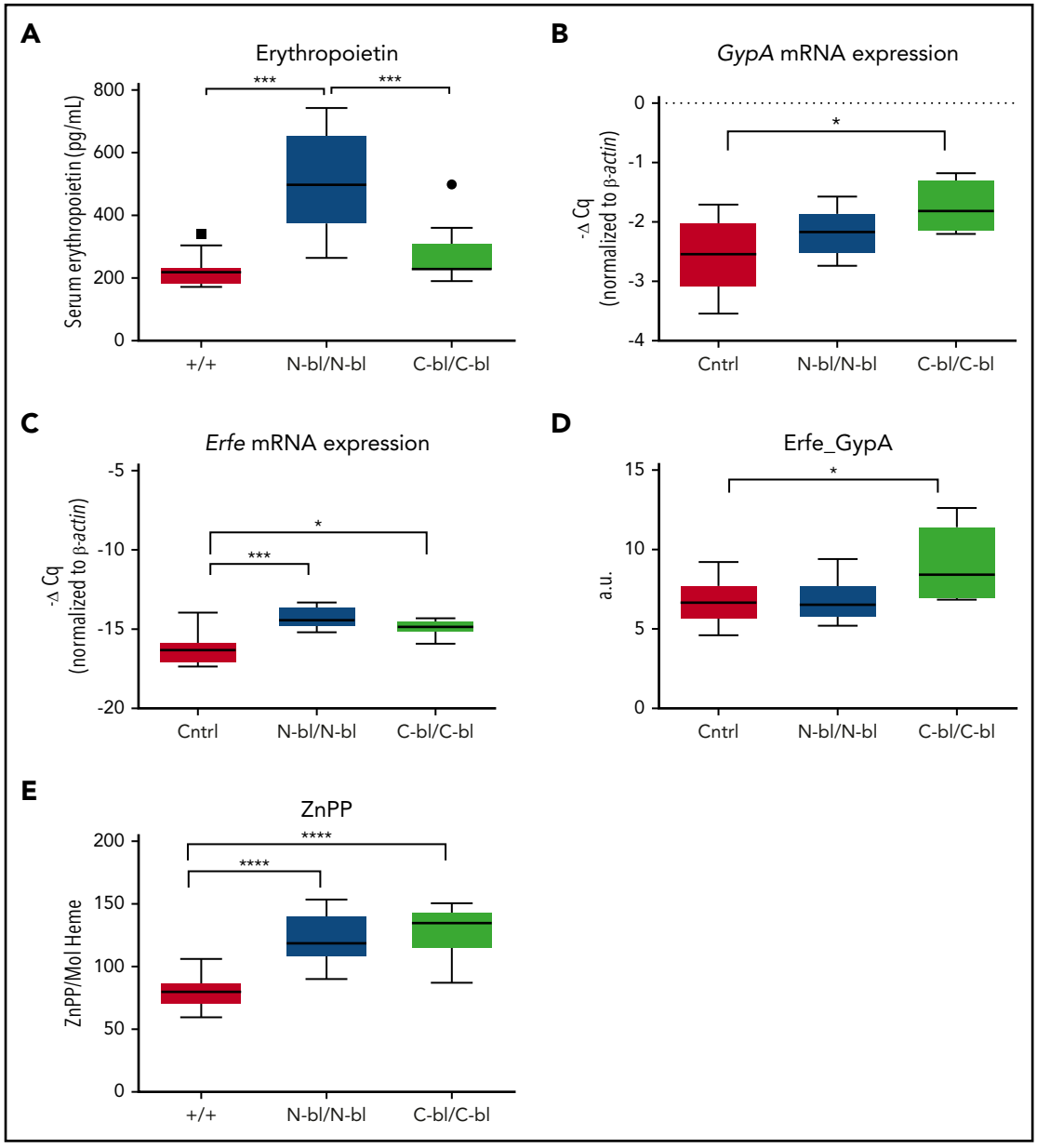

Figure 3. Iron binding to different lobes of Tf differentially affects erythropoietin levels despite similar erythroid signaling and iron availability for heme synthesis. (A) Serum Epo concentrations were significantly elevated in $Tf^{N\text{-}bl/N\text{-}bl}$ mice relative to both $Tf^{C\text{-}bl/C\text{-}bl}$ and WT mice (n = 5 mice per sex for each mutant strain and n = 10 mice per sex for WT). (B) $Tf^{C\text{-}bl/C\text{-}bl}$ mice showed significant increases in GypA messenger RNA (mRNA) levels relative to control mice (n = 4-7 mice per sex for WT and n = 3 mice per sex for mutant mice). (C) Erythroferrone (Erfe) mRNA levels were significantly higher in both $Tf^{N\text{-}bl/N\text{-}bl}$ and $Tf^{C\text{-}bl/C\text{-}bl}$ mice compared with controls (n = 4-7 mice per sex for WT and n = 3 mice per sex for mutant mice). (D) Upon normalization to GypA, Erfe expression was significantly higher in the $Tf^{C\text{-}bl/C\text{-}bl}$ mice relative to controls (n = 4-7 mice per sex for WT and n = 3 mice per sex for mutant mice). (E) $Tf^{N\text{-}bl/N\text{-}bl}$ and $Tf^{C\text{-}bl/C\text{-}bl}$ mice demonstrated elevated zinc protoporphyrin (ZnPP) concentrations per mole of heme (n = 9-7 mice per sex for WT and n = 5-8 mice per sex for mutant mice). Data are presented as Tukey box and whisker plots, with statistical significance analyzed by 1-way ANOVA. $^*P \leq .05$, $^{***}P \leq .001$, $^{****}P \leq .0001$.

mice were below the limit of detection by enzyme-linked immunosorbent assay (Elizabeta Nemeth, University of California, Los Angeles, e-mail, 11 April 2017). We also investigated iron availability for heme synthesis, as evidenced by the incorporation of zinc rather than iron into the protoporphyrin ring. Significant increases in zinc protoporphyrin were observed in both $Tf^{C\text{-}bl/C\text{-}bl}$ and $Tf^{N\text{-}bl/N\text{-}bl}$ relative to WT mice, but without differences between mutant strains (Figure 3E). Therefore, the loss of iron binding to either lobe of Tf was associated with decreased iron for heme production. However, the 2 mutant strains differed in circulating Epo levels and their Erfe expression profiles, suggesting differential Epo responsiveness.

Absence of iron in the N lobe of Tf is associated with decreased phosphorylation of the Epo target AKT

To investigate the possibility that the erythroid phenotype of the mutant strains arises from alterations in erythroid maturation or apoptosis, we analyzed bone marrow erythroid precursor populations by flow cytometry.[24] Data indicated no significant differences between strains in the percentages of erythroid

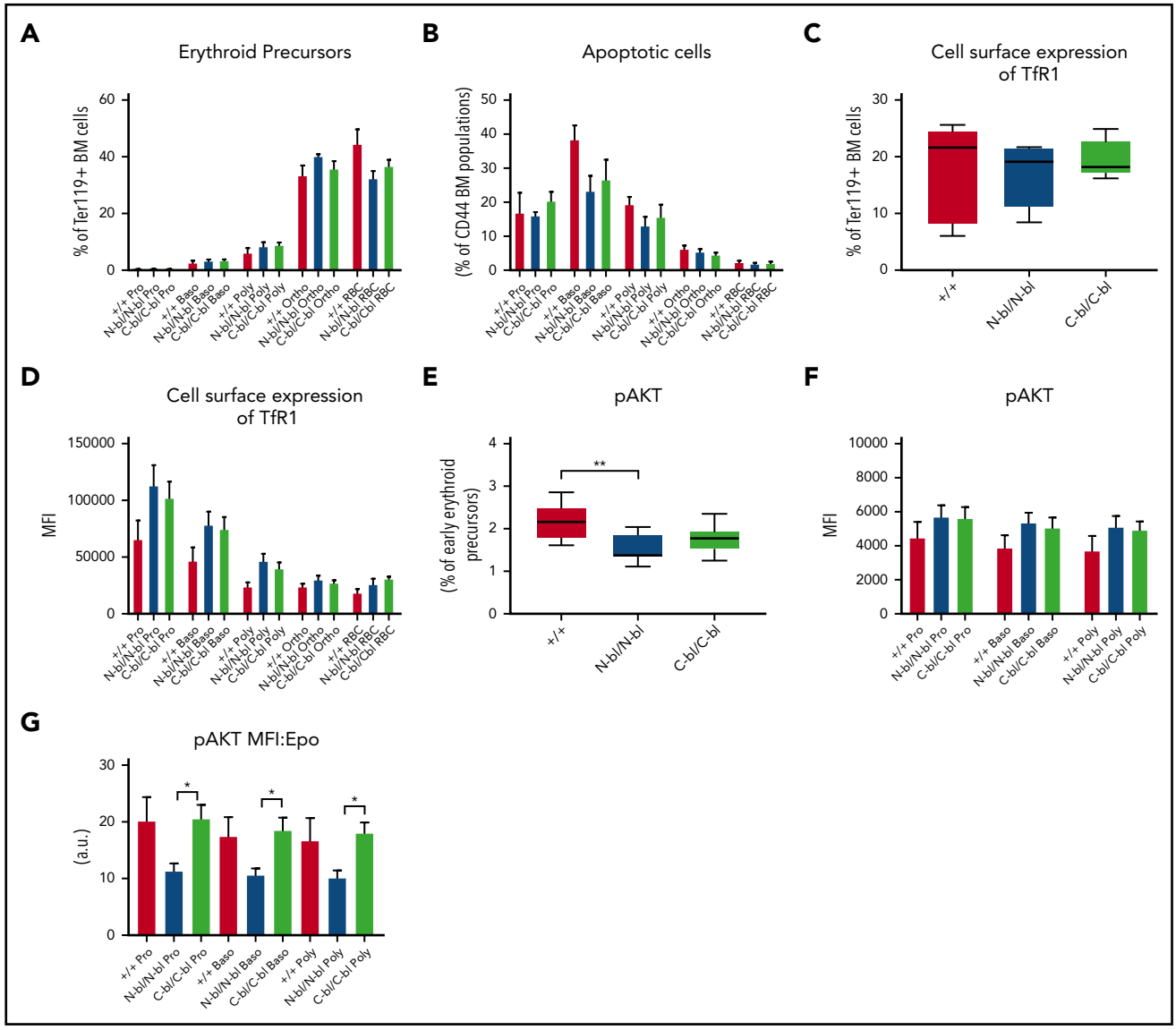

Figure 4. Differential erythroid effects of monoferric Tfs are associated with increased phosphorylation of the erythropoietin target AKT in early erythroid precursors. Flow cytometry analyses demonstrated no significant differences between strains in the relative proportion of erythroid precursor populations (A), no differences between strains in the percentages of apoptotic erythroid precursor cells (B), no significant differences in the percentages of erythroid lineage cells expressing cell-surface TfR1 (C), no significant differences in the median fluorescence intensity (MFI) of TfR1 in erythroid precursor populations (D), decreased percentages of cells positive for pAKT in early bone marrow (BM) erythroid precursor populations (proerythroblasts [Pro], basophilic [Baso] and polychromatic [Poly] erythroblasts) in the $Tf^{N\text{-}bl/N\text{-}bl}$ strain compared with WT (E), no significant differences in MFI of pAKT in early erythroid precursors between strains (F), and significantly decreased MFI of pAKT in $Tf^{N\text{-}bl/N\text{-}bl}$ mice compared with $Tf^{C\text{-}bl/C\text{-}bl}$ mice upon normalization to serum Epo concentrations (G). Data are presented as bar graphs depicting the mean ± standard error of the mean or Tukey box and whisker plots, with statistical significance analyzed by 1-way ANOVA (n = 4-5 mice per sex for WT and n = 5-7 mice per sex for Tf-mutant mice). $*P \leq .05$, $**P \leq .01$. Ortho, orthochromatic erythroblast.

precursor populations or in the percentages of early apoptotic (annexin V^+ 7-AAD^-) cells in each population (Figure 4A-B; supplemental Figure 7D). Analysis of cell-surface expression of TfR1 (CD71) in erythroid lineage ($Ter119^+$) bone marrow cells also indicated no differences in the percentages of positive cells between strains (Figure 4C). However, there was a trend toward increased expression in the Tf-mutant strains when the median fluorescence intensity of TfR1 was analyzed in erythroid progenitor populations (Figure 4D). Because phosphorylation of AKT is an Epo-mediated event that promotes erythroid precursor differentiation and survival,[36-38] we analyzed the percentage of pAKT in combined proerythroblast and basophilic and polychromatic erythroblast populations from the bone marrow. Results demonstrated a decreased percentage of $pAKT^+$ cells in $Tf^{N\text{-}bl/N\text{-}bl}$ mice relative to WT mice (Figure 4E). A trend toward increased expression in the Tf-mutant mice may have been evident when the median fluorescence intensity of pAKT was analyzed in the individual precursor populations (Figure 4F). However, when data were normalized to serum Epo concentrations, the level of pAKT remained significantly lower in the $Tf^{N\text{-}bl/N\text{-}bl}$ mice compared with the $Tf^{C\text{-}bl/C\text{-}bl}$ mice (Figure 4G). Overall, these data provide additional evidence for modulation of Epo responsiveness mediated by the iron status of the N lobe of Tf.

Mice with Tf-bound iron restricted to the N lobe have enhanced responsiveness to exogenous Epo

To further investigate Epo responsiveness, we treated $Tf^{C\text{-}bl/C\text{-}bl}$ and $Tf^{N\text{-}bl/N\text{-}bl}$ mice with exogenous Epo. RBC counts were

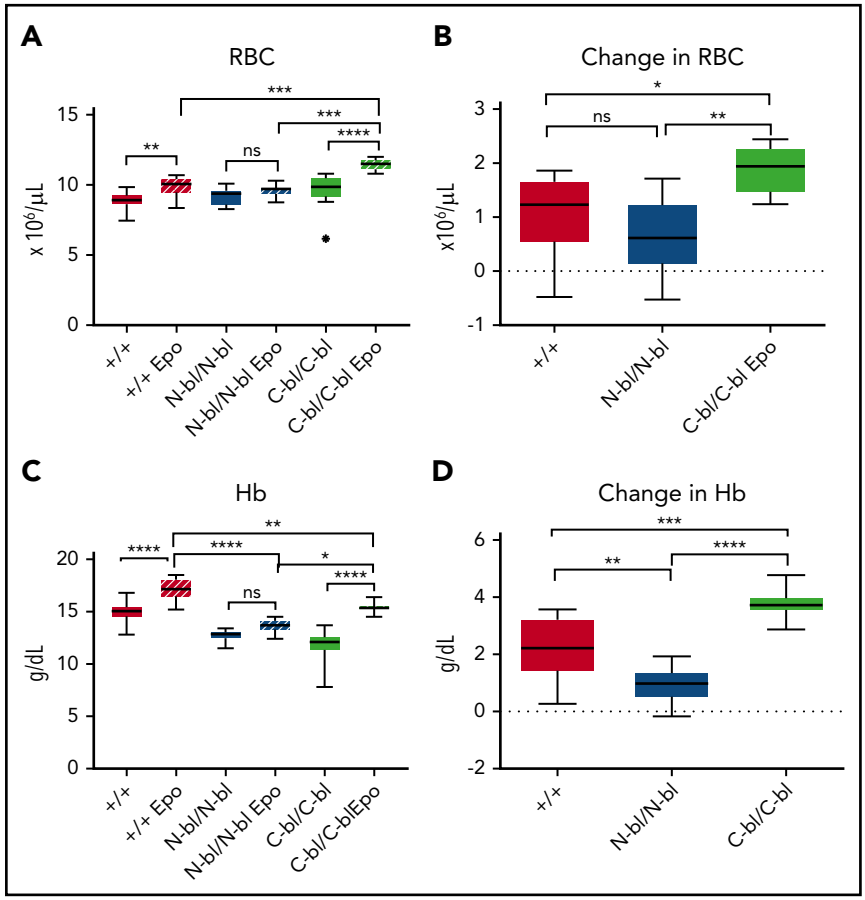

Figure 5. N lobe–bound iron enhances erythropoietin responsiveness. (A) Complete blood cell parameters from mice treated with 3000 IU/kg per day of recombinant human Epo demonstrated increased RBC counts in WT and $Tf^{C\text{-}bl/C\text{-}bl}$ mice but not in $Tf^{N\text{-}bl/N\text{-}bl}$ mice treated with Epo relative to controls (for saline-treated mice, n = 8-12 mice per sex for WT and n = 3-6 mice per sex for mutant mice; for Epo-treated mice, n = 6-9 mice per sex for WT and n = 4-5 mice per sex for mutant mice). (B) In response to Epo treatment, the change in RBCs, as measured by subtracting the average RBC count of respective saline-treated controls, was increased in $Tf^{C\text{-}bl/C\text{-}bl}$ mice compared with WT and $Tf^{N\text{-}bl/N\text{-}bl}$ mice (n = 4-6 mice per sex for each strain). (C) Hb concentrations in mice treated with Epo relative to controls showed significant increases in Hb concentration in WT and $Tf^{C\text{-}bl/C\text{-}bl}$ mice (for saline-treated mice, n = 8 mice per sex for WT and n = 3-6 mice per sex for mutant mice; for Epo-treated mice, n = 6-7 mice per sex for WT and n = 4-7 mice per sex for mutant mice). (D) In response to Epo treatment, the change in Hb, as measured by subtracting the average Hb of respective saline-treated controls, was greater in WT and $Tf^{C\text{-}bl/C\text{-}bl}$ mice than in $Tf^{N\text{-}bl/N\text{-}bl}$ mice, with a more substantial increase in the $Tf^{C\text{-}bl/C\text{-}bl}$ mice (n = 6-10 mice per sex for WT and n = 3-5 mice per sex for mutant mice). Data are presented as Tukey box and whisker plots. Statistical significance was analyzed by 1-way ANOVA. *$P \leq .05$, **$P \leq .01$, ***$P \leq .001$, ****$P \leq .0001$.

significantly higher only in Epo-treated $Tf^{C\text{-}bl/C\text{-}bl}$ and WT mice compared with saline-injected littermates (Figure 5A). Response to Epo in $Tf^{C\text{-}bl/C\text{-}bl}$ mice was even more robust than that in WT mice, with a significantly greater incremental change in RBC counts in Epo-treated $Tf^{C\text{-}bl/C\text{-}bl}$ relative to both Epo-treated $Tf^{N\text{-}bl/N\text{-}bl}$ and WT mice (Figure 5A-B). Hb was likewise significantly increased in Epo-treated compared with saline-injected $Tf^{C\text{-}bl/C\text{-}bl}$ and WT mice (Figure 5C). This change in Hb, as determined by subtracting from the average value of saline-treated controls, was significantly greater in WT and $Tf^{C\text{-}bl/C\text{-}bl}$ mice than in $Tf^{N\text{-}bl/N\text{-}bl}$ mice (Figure 5D). No significant increase in RBC counts or Hb was evident in $Tf^{N\text{-}bl/N\text{-}bl}$ mice in response to exogenous Epo (Figure 5A-D). The findings in the $Tf^{N\text{-}bl/N\text{-}bl}$ mice were similar to those observed in certain hypoproliferative anemias (ie, increased baseline Epo levels and poor responsiveness to exogenous Epo).[39]

As expected with induction of extramedullary hematopoiesis, the splenic weight index was increased after Epo treatment in all strains (supplemental Figure 5C). The magnitude of increase was significantly smaller in $Tf^{N\text{-}bl/N\text{-}bl}$ mice compared with Epo-treated WT mice (supplemental Figure 5C). MCH remained decreased in the Tf-mutant strains compared with WT mice (supplemental Figure 5A). Reticulocyte counts showed a significant increase in response to Epo treatment in WT and $Tf^{C\text{-}bl/C\text{-}bl}$ mice but not in $Tf^{N\text{-}bl/N\text{-}bl}$ mice (supplemental Figure 5B). Thus, the $Tf^{C\text{-}bl/C\text{-}bl}$ mice demonstrated enhanced Epo responsiveness despite other evidence of iron-restricted erythropoiesis. These observations suggest that a normal iron restriction response depends on loss of iron binding to the N lobe (or iron occupancy of the C lobe) of Tf.

Monoferric Tf strains manifest a hemochromatosis phenotype that is more pronounced with absence of iron binding in the N compared with C lobe

We next examined whether the loss of iron binding to the N or C lobe of Tf has differential effects on tissue iron parameters and hepcidin signaling. Both $Tf^{C\text{-}bl/C\text{-}bl}$ and $Tf^{N\text{-}bl/N\text{-}bl}$ mice had significant increases in hepatic iron concentrations compared with WT mice, with a greater increase in $Tf^{N\text{-}bl/N\text{-}bl}$ relative to $Tf^{C\text{-}bl/C\text{-}bl}$ mice (Figure 6A). Perls' staining of liver sections showed iron overload with hepatocellular distribution in both mutant mice, with a more zonal distribution in the $Tf^{C\text{-}bl/C\text{-}bl}$ mice (Figure 6B; supplemental Figure 6A,C). Splenic iron concentrations were decreased in both mutant strains relative to WT mice (Figure 6C-D; supplemental Figure 6B,D). The hepatic iron loading and splenic iron sparing were consistent with dysregulation of hepcidin and led us to investigate serum hepcidin and liver hepcidin (*Hamp1*) mRNA levels. Serum hepcidin was lower in both $Tf^{C\text{-}bl/C\text{-}bl}$ and $Tf^{N\text{-}bl/N\text{-}bl}$ mice; however, only the $Tf^{N\text{-}bl/N\text{-}bl}$ mice were significantly different from WT mice (Figure 6E). Hepatic *Hamp1* mRNA data showed the same profile (supplemental Figure 6). Upon normalization to liver iron concentration, serum hepcidin levels were significantly lower than WT in both strains and higher in the $Tf^{C\text{-}bl/C\text{-}bl}$ relative to the $Tf^{N\text{-}bl/N\text{-}bl}$ mice (Figure 6F). Despite the substantially increased hepatic iron concentrations in both mutants, significant differences were not detected in hepatic *Bmp6* or *Bmp2* expression

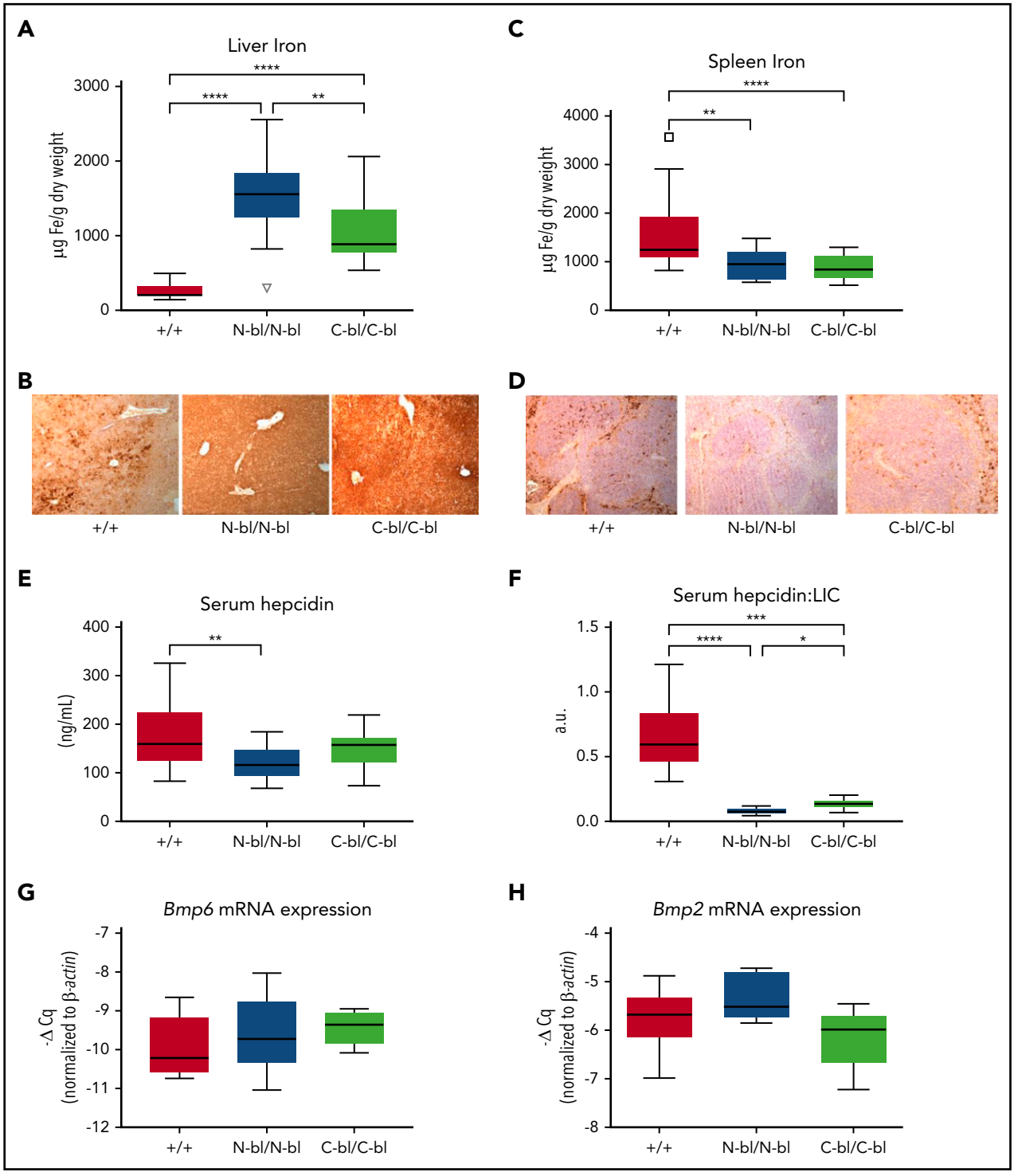

Figure 6. Monoferric strains produce a hemochromatosis phenotype that is more pronounced upon loss of iron binding in the N lobe. (A) Hepatic iron concentrations were significantly higher in the $Tf^{N\text{-}bl/N\text{-}bl}$ strain than in the $Tf^{C\text{-}bl/C\text{-}bl}$ strain and higher in both mutant strains than in WT (n = 9-10 mice per sex). (B) Enhanced Perls' staining showed higher iron in the $Tf^{N\text{-}bl/N\text{-}bl}$ and $Tf^{C\text{-}bl/C\text{-}bl}$ mice compared with WT. (C) Splenic iron concentrations were significantly lower in both the $Tf^{N\text{-}bl/N\text{-}bl}$ and the $Tf^{C\text{-}bl/C\text{-}bl}$ mice than in WT mice (n = 10-12 mice per sex). (D) Enhanced Perls' staining confirmed decreased splenic iron in the $Tf^{N\text{-}bl/N\text{-}bl}$ and $Tf^{C\text{-}bl/C\text{-}bl}$ mice compared with WT littermates. (E) Serum hepcidin levels were decreased in the $Tf^{N\text{-}bl/N\text{-}bl}$ mice compared with WT (n = 11 WT females and n = 4-7 females for each mutant strain). (F) Upon normalization to mean liver iron concentrations (LICs) for each strain, serum hepcidin values were significantly lower in both Tf-mutant strains compared with WT and significantly lower in the $Tf^{N\text{-}bl/N\text{-}bl}$ strain compared with the $Tf^{C\text{-}bl/C\text{-}bl}$ strain. Quantitative PCR data, presented as the fold change in expression relative to β-actin, demonstrated no significant differences in *Bmp6* mRNA levels (n = 8-10 mice per sex) (G) or *Bmp2* mRNA expression (n = 3-4 mice per sex) (H). Data are presented as Tukey box and whisker plots. Statistical significance was analyzed by Kruskal-Wallis test or 1-way ANOVA. $*P \leq .05$, $**P \leq .01$, $***P \leq .001$, $****P \leq .0001$.

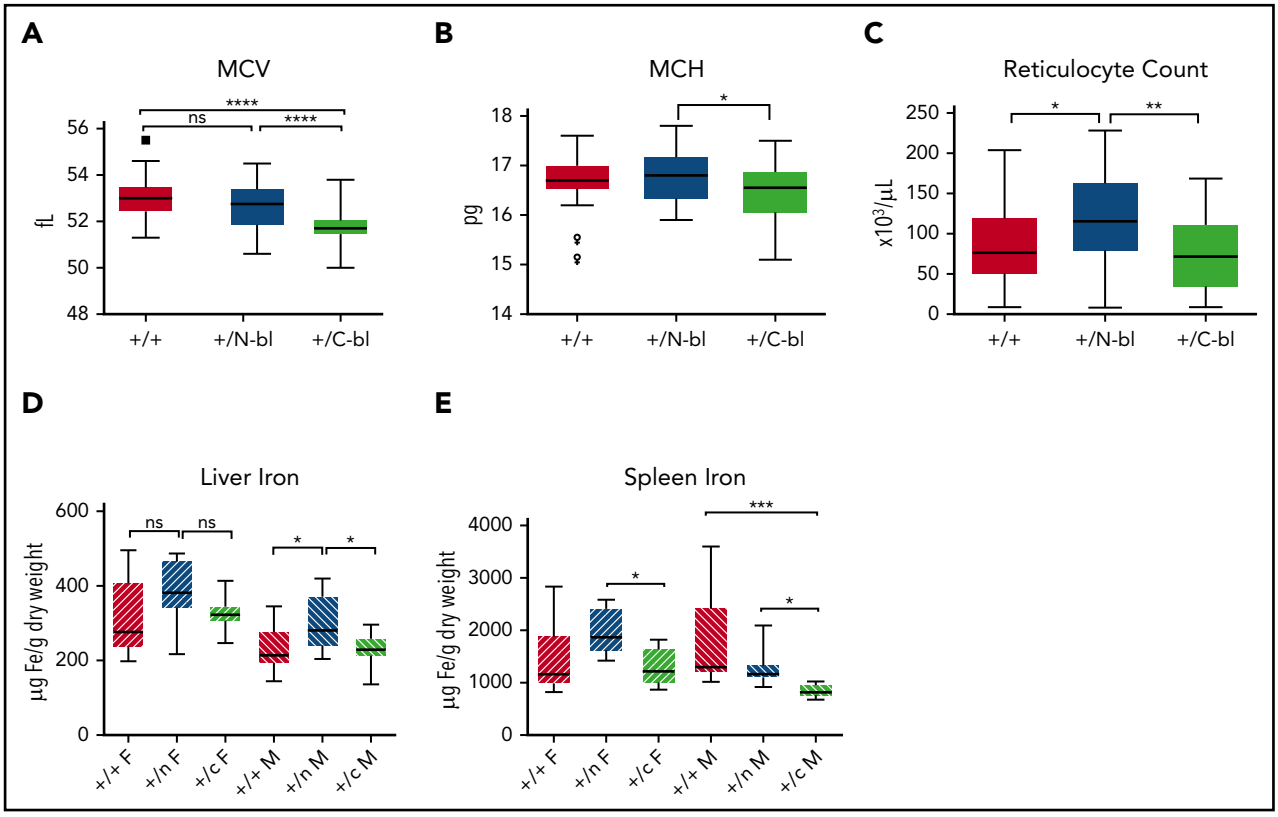

Figure 7. The phenotype of heterozygous mice subtly mirrors much of the homozygous phenotype. Complete blood count parameters (n = 15-17 mice per sex) demonstrated significant decreases in MCV in the $Tf^{C\text{-}bl/+}$ mice relative to $Tf^{N\text{-}bl/+}$ or WT mice (A), significant decreases in MCH in $Tf^{C\text{-}bl/+}$ mice relative to $Tf^{N\text{-}bl/+}$ mice (B), and significant increases in reticulocyte count in the $Tf^{N\text{-}bl/+}$ mice relative to both $Tf^{C\text{-}bl/+}$ and WT mice (C). Tissue iron assays (n = 9-11 mice per sex) demonstrated a significant increase in hepatic iron concentration in the $Tf^{N\text{-}bl/+}$ male mice relative to $Tf^{C\text{-}bl/+}$ and WT male mice (D) and significant decreases in splenic iron in the $Tf^{C\text{-}bl/+}$ females compared with $Tf^{N\text{-}bl/+}$females and in $Tf^{C\text{-}bl/+}$ males relative to both $Tf^{N\text{-}bl/+}$ males and WT males (E). Data are presented as Tukey box and whisker plots. Statistical significance was analyzed by Kruskal-Wallis or 1-way ANOVA. $*P \leq .05$, $**P \leq .01$, $***P \leq .001$, $****P \leq .0001$.

(Figure 6G-H). The greater hepatic iron loading in $Tf^{N\text{-}bl/N\text{-}bl}$ relative to $Tf^{C\text{-}bl/C\text{-}bl}$ mice was thus associated with lower hepcidin expression and supports a model in which Tf-mediated signaling to hepcidin is influenced by lobe-specific iron occupancy.

Heterozygosity for monoferric N vs C lobe Tf differentially affects iron metabolism and erythropoiesis

We analyzed heterozygous Tf lobe–mutant mice to determine if alterations in the distribution of monoferric N and C Tf would have phenotypic effects in the presence of a normal Tf allele. Indeed, many of the erythropoietic alterations observed in homozygous mutants were subtly recapitulated in heterozygotes. Specifically, MCV was decreased in $Tf^{C\text{-}bl/+}$ mice compared with $Tf^{N\text{-}bl/+}$ and WT mice (Figure 7A). $Tf^{C\text{-}bl/+}$ mice demonstrated decreased MCH compared with $Tf^{N\text{-}bl/+}$ mice (Figure 7B). $Tf^{N\text{-}bl/+}$ mice demonstrated a modest increase in reticulocyte counts compared with WT mice; they were also higher than those in $Tf^{C\text{-}bl/+}$ mice (Figure 7C). The hepatic iron concentration was significantly higher in male $Tf^{N\text{-}bl/+}$ mice relative to male WT and $Tf^{C\text{-}bl/+}$ mice (Figure 7D). Lastly, splenic iron concentrations were lower in $Tf^{C\text{-}bl/+}$ mice compared with $Tf^{N\text{-}bl/+}$ and WT mice in males and with $Tf^{N\text{-}bl/+}$ mice in females (Figure 7E). These data suggest that even in the presence of diferric Tf, alterations in the distribution of iron across N and C lobes modulate erythropoietic indices and iron metabolism.

Discussion

Differences in physical, structural, and metal-binding properties between the 2 Tf lobes have led to considerable interest in potential functional consequences. Early studies suggesting that iron delivery to reticulocytes[2] is specific to the Tf C lobe led to the Fletcher-Huehns hypothesis[40] that circulating N vs C monoferric Tf levels reflect tissue-specific utilization patterns and may serve to regulate iron homeostasis. Indeed, the proportion of the 2 monoferric forms in humans is unequal and varies with iron status.[41] However, subsequent ex vivo and animal studies testing the Fletcher-Huehns hypothesis yielded inconsistent results, and interest in the monoferric forms dissipated when they were found to compete poorly with diferric Tf for binding to TfR1. As such, evidence for the physiologic relevance of each of the 2 Tf lobes has remained lacking. Observations in the $Tf^{N\text{-}bl}$ and $Tf^{C\text{-}bl}$ mice provide such evidence.

The $Tf^{N\text{-}bl/N\text{-}bl}$ and $Tf^{C\text{-}b/C\text{-}bl}$ mice both had decreased iron availability for erythroid heme production, as manifested in elevated zinc protoporphyrin levels and microcytic anemia. Although not surprising, in that the monoferric forms can deliver only 1 iron molecule per TfR1 cycle, it also indicates that the erythroid precursors were unable to compensate by, for example, an increase in receptor number. The lack of evidence for systemic iron deficiency (ie, normal growth, similar TfR1 protein levels), moreover, suggests that a shift toward monoferric forms might

provide a mechanism for decreasing erythroid iron utilization for heme when needed for other purposes.

Importantly, the phenotype of the Tf lobe–mutant mice cannot be attributed simply to decreased iron delivery, because it did not mimic other models in which Tf-mediated iron delivery is impaired. The mutant mice differed from mice with dietary iron deficiency by increased rather than decreased liver iron and (in the case of the $Tf^{C\text{-}bl/C\text{-}bl}$ mice) by increased RBC counts rather than erythropenia. They differed from TfR1 hemizygous mice by decreases in hepcidin and hepatic iron loading and absence of reticulocytosis.[33,42] Although direct comparison was not possible, Epo responsiveness was unlikely to be different in the TfR1 hemizygous mice, because the hemoglobin concentration was ~97% of its control.[33] Although the $Tf^{C\text{-}bl/C\text{-}bl}$ mice demonstrated some similarities to the TfR1 hemizygous strain, including increased RBC counts and slightly decreased Hb levels, the $Tf^{N\text{-}bl/N\text{-}bl}$ mice differed from both by a lack of increase in circulating RBCs despite increased serum Epo levels and anemia. Homozygous hypotransferrinemic mice demonstrated marked erythropenia, massive splenomegaly, and pronounced reticulocytosis,[43] which were not seen in Tf lobe–mutant mice. Findings in the Tf lobe–mutant mice suggest specific roles for monoferric forms of Tf beyond iron delivery for heme, to include regulation of hepcidin expression and Epo sensitivity.

There are several possible contributors to the observed hepcidin suppression (Figure 6E; supplemental Figure 6) and hepatic iron loading (Figure 6A-B) in the Tf lobe–mutant mice. TfR2 is a mediator of hepatic hepcidin regulation in response to iron status.[44-46] Possibly, diferric Tf is more effective than either monoferric form in hepatocellular TfR2-mediated upregulation of hepcidin. As Tf saturations fall and monoferric forms increasingly predominate over diferric, they could plausibly compete for TfR2 occupancy and attenuate hepcidin expression. Differences in liver iron loading between the $Tf^{N\text{-}bl}$ and $Tf^{C\text{-}bl}$ mice suggest that iron occupancy of the N lobe may make transferrin a more effective hepcidin upregulatory signaling molecule. These differences were seen in homozygous (Figure 6A-B) as well as heterozygous (Figure 7D, male) mice. The latter observation supports a role for the monoferric forms of Tf in iron homeostasis, even in the presence of diferric Tf and in the absence of anemia. The lack of an increase in liver *Bmp6* and *Bmp2* expression in the mutant mice (Figure 6G-H), despite liver iron loading, raises the possibility that Tf contributes to sinusoidal *Bmp6* expression.[47] Erfe is an important downregulator of hepcidin in iron-loading anemias[35]; however, Erfe mRNA was only modestly increased in the marrow of the Tf-mutant mice (Figure 3C), and serum levels remained undetectable.

Observations in the Tf lobe–mutant mice demonstrated specific roles for each monoferric form in the regulation of Epo sensitivity. Epo promotes erythroid precursor survival, proliferation, and differentiation when iron is sufficient.[48,49] However, in iron deficiency, erythroblasts are relatively resistant to Epo, contributing to hypoproliferative anemia. Our observations suggest that Tf lobe–specific iron occupancy influences Epo responsiveness.

Although it is possible that the observed phenotypes were mediated by TfR1, we speculate that the effects of the monoferric Tfs on Epo sensitivity were mediated via TfR2. TfR2 partners with the EpoR in erythroid precursors, with consequences on EpoR availability and/or stability.[14,16,32,50-52] Mice receiving transplants of $TfR2^{-/-}$ bone marrow did not develop anemia or further suppress hepcidin on an iron-deficient diet,[15] strongly suggesting that erythroid TfR2 is required for the iron restriction response.[16,32,50] Supporting a role for specificity of the Tf lobe iron occupancy in this regulation are the striking similarities in the erythroid phenotype between the $Tf^{C\text{-}bl/C\text{-}bl}$ mice reported here and the TfR2 bone marrow knockout mice on a low-iron diet.[15] Both of these models failed to demonstrate the blunting of Epo responsiveness anticipated with iron-deficient erythropoiesis. Both of these models contrasted with the $Tf^{N\text{-}bl/N\text{-}bl}$ mice, where iron-limited heme production was associated with expected suppression of Epo responsiveness.

Heterozygous N and C Tf lobe–mutant mice differed from WT mice and from each other, suggesting that changes in the relative concentrations of N and C monoferric Tfs influence iron metabolism and erythropoiesis, even in the presence of diferric Tf. On the basis of these data, we speculate that iron occupancy of the N lobe (including diferric Tf) would serve to indicate relative circulating iron sufficiency. This model is supported further by the preferential loading of iron initially onto the C lobe of apotransferrin (facilitated by binding to ceruloplasmin)[53] and subsequent cooperative loading of iron onto the N lobe[54] when available.

The studies presented here demonstrate that monoferric forms of Tf are functionally important and functionally distinct. These mice provide evidence of participation of the monoferric Tf forms as signaling molecules in regulating hepcidin and Epo responsiveness. The recent report that loss of erythroid TfR2 increases Epo sensitivity and improves erythropoiesis in murine thalassemia minor[55] raises the possibility of reproducing that effect in the presence of TfR2 using C-blocked Tf. Moreover, measuring Tf forms in settings of Epo resistance may be informative.

Acknowledgments

The authors thank Tomaz Ganz and Elizabeta Nemeth at University of California Los Angeles for measurements of zinc protoporphyrin and serum Erfe, as well as for helpful discussions regarding these studies; Eldad Hod at Columbia University School of Medicine for NTBI measurements; Nisha A. George and Shivam Bhanvadia for technical assistance; and Sukanya Suresh for helpful discussions on erythropoietin responsiveness.

This work was supported in part by grants R01DK095112 (S.R., Y.Z.G., and R.E.F.), 5RO1DK090554-07 (S.R.), and R01DK107670 (Y.Z.G.) from the National Institute of Diabetes and Digestive and Kidney Diseases, National Institutes of Health (NIH); NIH Clinical and Translational Science Award UL1 TR002345 (N.L.P. and R.E.F.); and grant 9168 (R.E.F.) from the Saint Louis University School of Medicine President's Research Fund.

Authorship

Contribution: R.E.F., Y.Z.G., and S.R. conceptualized the study; R.E.F. and S.R. were responsible for methodology; N.L.P., Y.L., M.F., A.G., C.C., P.P., L.M., F.A., E.V., and R.E.F. performed investigations; R.E.F., S.R., Y.Z.G., and N.L.P. performed formal analyses; R.E.F., N.L.P., S.R., and Y.Z.G. wrote the original draft; R.E.F., Y.Z.G., and S.R. were responsible for funding acquisition; and R.E.F. acted as supervisor.

Conflict-of-interest disclosure: R.E.F. is a member of the scientific advisory board of Protagonist Therapeutics. Y.Z.G. serves as a consultant for Ionis Pharmaceuticals, is a member of the scientific advisory board of LaJolla Pharmaceutical Company (LJPC), and receives funding from ApoPharma. S.R. receives funding from Ionis Pharmaceuticals and is a member of its scientific advisory board, is a consultant for Protagonist Therapeutics, LJPC, and Disc Medicine, and is a member of the advisory board of Meira GTx. The remaining authors declare no competing financial interests.

ORCID profiles: A.G., 0000-0002-6602-1854; L.M., 0000-0001-9920-7308; S.R., 0000-0002-0938-6558; Y.Z.G., 0000-0002-3496-3783; R.E.F., 0000-0003-0154-4483.

Correspondence: Robert E. Fleming, Saint Louis University School of Medicine, Room 217, Doisy Research Building, 1100 S Grand Blvd, St. Louis, MO 63104; e-mail: robert.fleming@health.slu.edu.

Footnotes

Submitted 20 December 2018; accepted 12 August 2019. Prepublished online as *Blood* First Edition paper, 21 August 2019; DOI 10.1182/blood.2018893099.

*S.R., Y.Z.G., and R.E.F. served as senior authors.

For original data, contact Robert Fleming (robert.fleming@health.slu.edu).

The online version of this article contains a data supplement.

There is a *Blood* Commentary on this article in this issue.

The publication costs of this article were defrayed in part by page charge payment. Therefore, and solely to indicate this fact, this article is hereby marked "advertisement" in accordance with 18 USC section 1734.

REFERENCES

1. Luck AN, Mason AB. Transferrin-mediated cellular iron delivery. *Curr Top Membr*. 2012; 69:3-35.
2. Bartnikas TB, Andrews NC, Fleming MD. Transferrin is a major determinant of hepcidin expression in hypotransferrinemic mice. *Blood*. 2011;117(2):630-637.
3. Lambert LA, Perri H, Meehan TJ. Evolution of duplications in the transferrin family of proteins. *Comp Biochem Physiol B Biochem Mol Biol*. 2005;140(1):11-25.
4. MacGillivray RT, Mendez E, Shewale JG, Sinha SK, Lineback-Zins J, Brew K. The primary structure of human serum transferrin. The structures of seven cyanogen bromide fragments and the assembly of the complete structure. *J Biol Chem*. 1983;258(6): 3543-3553.
5. Makey DG, Seal US. The detection of four molecular forms of human transferrin during the iron binding process. *Biochim Biophys Acta*. 1976;453(1):250-256.
6. DiRusso SC, Check IJ, Hunter RL. Quantitation of apo-, mono-, and diferric transferrin by polyacrylamide gradient gel electrophoresis in patients with disorders of iron metabolism. *Blood*. 1985;66(6):1445-1451.
7. Huebers HA, Csiba E, Huebers E, Finch CA. Competitive advantage of diferric transferrin in delivering iron to reticulocytes. *Proc Natl Acad Sci USA*. 1983;80(1):300-304.
8. Tong X, Kawabata H, Koeffler HP. Iron deficiency can upregulate expression of transferrin receptor at both the mRNA and protein level. *Br J Haematol*. 2002;116(2):458-464.
9. Coulon S, Dussiot M, Grapton D, et al. Polymeric IgA1 controls erythroblast proliferation and accelerates erythropoiesis recovery in anemia. *Nat Med*. 2011;17(11): 1456-1465.
10. Kenneth NS, Mudie S, Naron S, Rocha S. TfR1 interacts with the IKK complex and is involved in IKK-NF-κB signalling. *Biochem J*. 2013; 449(1):275-284.
11. Wallace DF, Summerville L, Crampton EM, Frazer DM, Anderson GJ, Subramaniam VN. Combined deletion of Hfe and transferrin receptor 2 in mice leads to marked dysregulation of hepcidin and iron overload. *Hepatology*. 2009;50(6):1992-2000.
12. Corradini E, Rozier M, Meynard D, et al. Iron regulation of hepcidin despite attenuated Smad1,5,8 signaling in mice without transferrin receptor 2 or Hfe. *Gastroenterology*. 2011;141(5):1907-1914.
13. Kawabata H, Nakamaki T, Ikonomi P, Smith RD, Germain RS, Koeffler HP. Expression of transferrin receptor 2 in normal and neoplastic hematopoietic cells. *Blood*. 2001;98(9): 2714-2719.
14. Forejtnikovà H, Vieillevoye M, Zermati Y, et al. Transferrin receptor 2 is a component of the erythropoietin receptor complex and is required for efficient erythropoiesis. *Blood*. 2010;116(24):5357-5367.
15. Nai A, Lidonnici MR, Rausa M, et al. The second transferrin receptor regulates red blood cell production in mice. *Blood*. 2015; 125(7):1170-1179.
16. Khalil S, Delehanty L, Grado S, et al. Iron modulation of erythropoiesis is associated with Scribble-mediated control of the erythropoietin receptor. *J Exp Med*. 2018;215(2): 661-679.
17. Chua AC, Trinder D, Olynyk JK. Liver and serum iron: discrete regulators of hepatic hepcidin expression. *Hepatology*. 2011;54(1): 16-19.
18. Corradini E, Meynard D, Wu Q, et al. Serum and liver iron differently regulate the bone morphogenetic protein 6 (BMP6)-SMAD signaling pathway in mice. *Hepatology*. 2011; 54(1):273-284.
19. Lin L, Valore EV, Nemeth E, Goodnough JB, Gabayan V, Ganz T. Iron transferrin regulates hepcidin synthesis in primary hepatocyte culture through hemojuvelin and BMP2/4. *Blood*. 2007;110(6):2182-2189.
20. Kleven MD, Jue S, Enns CA. Transferrin receptors TfR1 and TfR2 bind transferrin through differing mechanisms. *Biochemistry*. 2018; 57(9):1552-1559.
21. Kawabata H, Germain RS, Vuong PT, Nakamaki T, Said JW, Koeffler HP. Transferrin receptor 2-alpha supports cell growth both in iron-chelated cultured cells and in vivo. *J Biol Chem*. 2000;275(22):16618-16625.
22. Li H, Rybicki AC, Suzuka SM, et al. Transferrin therapy ameliorates disease in beta-thalassemic mice. *Nat Med*. 2010;16(2): 177-182.
23. Mason AB, Halbrooks PJ, Larouche JR, et al. Expression, purification, and characterization of authentic monoferric and apo-human serum transferrins. *Protein Expr Purif*. 2004; 36(2):318-326.
24. Chen K, Liu J, Heck S, Chasis JA, An X, Mohandas N. Resolving the distinct stages in erythroid differentiation based on dynamic changes in membrane protein expression during erythropoiesis. *Proc Natl Acad Sci USA*. 2009;106(41):17413-17418.
25. Gardenghi S, Ramos P, Marongiu MF, et al. Hepcidin as a therapeutic tool to limit iron overload and improve anemia in β-thalassemic mice. *J Clin Invest*. 2010; 120(12):4466-4477.
26. Hod EA, Zhang N, Sokol SA, et al. Transfusion of red blood cells after prolonged storage produces harmful effects that are mediated by iron and inflammation. *Blood*. 2010;115(21): 4284-4292.
27. Carter P. Spectrophotometric determination of serum iron at the submicrogram level with a new reagent (ferrozine). *Anal Biochem*. 1971; 40(2):450-458.
28. Torrance JD, Bothwell TH. Tissue iron stores. In: Cook JD, ed. Iron, New York, NY: Churchill Livingstone; 1980:90-115.
29. Livak KJ, Schmittgen TD. Analysis of relative gene expression data using real-time quantitative PCR and the 2(-Delta Delta C(T)) Method. *Methods*. 2001;25(4):402-408.
30. Tomatsu S, Orii KO, Fleming RE, et al. Contribution of the H63D mutation in HFE to murine hereditary hemochromatosis. *Proc Natl Acad Sci USA*. 2003;100(26): 15788-15793.
31. Batey RG, Lai Chung Fong P, Shamir S, Sherlock S. A non-transferrin-bound serum iron in idiopathic hemochromatosis. *Dig Dis Sci*. 1980;25(5):340-346.
32. Wallace DF, Secondes ES, Rishi G, et al. A critical role for murine transferrin receptor 2 in erythropoiesis during iron restriction. *Br J Haematol*. 2015;168(6):891-901.
33. Levy JE, Jin O, Fujiwara Y, Kuo F, Andrews NC. Transferrin receptor is necessary for development of erythrocytes and the nervous system. *Nat Genet*. 1999;21(4):396-399.
34. Gahmberg CG, Jokinen M, Andersson LC. Expression of the major sialoglycoprotein

(glycophorin) on erythroid cells in human bone marrow. *Blood*. 1978;52(2):379-387.

35. Kautz L, Jung G, Valore EV, Rivella S, Nemeth E, Ganz T. Identification of erythroferrone as an erythroid regulator of iron metabolism. *Nat Genet*. 2014;46(7):678-684.

36. Bouscary D, Pene F, Claessens YE, et al. Critical role for PI 3-kinase in the control of erythropoietin-induced erythroid progenitor proliferation. *Blood*. 2003;101(9):3436-3443.

37. Zhao W, Kitidis C, Fleming MD, Lodish HF, Ghaffari S. Erythropoietin stimulates phosphorylation and activation of GATA-1 via the PI3-kinase/AKT signaling pathway. *Blood*. 2006;107(3):907-915.

38. Bao H, Jacobs-Helber SM, Lawson AE, Penta K, Wickrema A, Sawyer ST. Protein kinase B (c-Akt), phosphatidylinositol 3-kinase, and STAT5 are activated by erythropoietin (EPO) in HCD57 erythroid cells but are constitutively active in an EPO-independent, apoptosis-resistant subclone (HCD57-SREI cells). *Blood*. 1999;93(11):3757-3773.

39. Cazzola M, Mercuriali F, Brugnara C. Use of recombinant human erythropoietin outside the setting of uremia. *Blood*. 1997;89(12):4248-4267.

40. Fletcher J, Huehns ER. Function of transferrin. *Nature*. 1968;218(5148):1211-1214.

41. Zak O, Aisen P. Nonrandom distribution of iron in circulating human transferrin. *Blood*. 1986;68(1):157-161.

42. Keel SB, Doty R, Liu L, et al. Evidence that the expression of transferrin receptor 1 on erythroid marrow cells mediates hepcidin suppression in the liver. *Exp Hematol*. 2015;43(6):469-478.e6.

43. Bernstein SE. Hereditary hypotransferrinemia with hemosiderosis, a murine disorder resembling human atransferrinemia. *J Lab Clin Med*. 1987;110(6):690-705.

44. Camaschella C, Roetto A, Calì A, et al. The gene TFR2 is mutated in a new type of haemochromatosis mapping to 7q22. *Nat Genet*. 2000;25(1):14-15.

45. Fleming RE, Ahmann JR, Migas MC, et al. Targeted mutagenesis of the murine transferrin receptor-2 gene produces hemochromatosis. *Proc Natl Acad Sci USA*. 2002;99(16):10653-10658.

46. Nemeth E, Roetto A, Garozzo G, Ganz T, Camaschella C. Hepcidin is decreased in TFR2 hemochromatosis. *Blood*. 2005;105(4):1803-1806.

47. Canali S, Zumbrennen-Bullough KB, Core AB, et al. Endothelial cells produce bone morphogenetic protein 6 required for iron homeostasis in mice. *Blood*. 2017;129(4):405-414.

48. Goldwasser E. Erythropoietin and the differentiation of red blood cells. *Fed Proc*. 1975;34(13):2285-2292.

49. Silva M, Grillot D, Benito A, Richard C, Nuñez G, Fernández-Luna JL. Erythropoietin can promote erythroid progenitor survival by repressing apoptosis through Bcl-XL and Bcl-2. *Blood*. 1996;88(5):1576-1582.

50. Rishi G, Secondes ES, Wallace DF, Subramaniam VN. Hematopoietic deletion of transferrin receptor 2 in mice leads to a block in erythroid differentiation during iron-deficient anemia. *Am J Hematol*. 2016;91(8):812-818.

51. Nai A, Pellegrino RM, Rausa M, et al. The erythroid function of transferrin receptor 2 revealed by Tmprss6 inactivation in different models of transferrin receptor 2 knockout mice. *Haematologica*. 2014;99(6):1016-1021.

52. Lee P, Hsu MH, Welser-Alves J, Peng H. Severe microcytic anemia but increased erythropoiesis in mice lacking Hfe or Tfr2 and Tmprss6. *Blood Cells Mol Dis*. 2012;48(3):173-178.

53. Eid C, Hémadi M, Ha-Duong NT, El Hage Chahine JM. Iron uptake and transfer from ceruloplasmin to transferrin. *Biochim Biophys Acta*. 2014;1840(6):1771-1781.

54. Pakdaman R, El Hage Chahine JM. A mechanism for iron uptake by transferrin. *Eur J Biochem*. 1996;236(3):922-931.

55. Artuso I, Lidonnici MR, Altamura S, et al. Transferrin receptor 2 is a potential novel therapeutic target for β-thalassemia: evidence from a murine model [published correction appears in Blood. 2019;134(1):94]. *Blood*. 2018;132(21):2286-2297.